Supplementary data

Bilayer hydrogel mimicking periosteum-bone structure for innervated bone regeneration

Wenhui Lyu, [a] *Yuyue Zhang,* [b] *Shaopei Ding,* [b] *Xiang Li,* [a] *Tong Sun,* [b] *Jun Luo,* [b] *Jian Wang,* [a] *Jianshu Li*[bcd] *and Lei Li*[a]*

[a]State Key Laboratory of Oral Diseases, National Center for Stomatology, National Clinical Research Center for Oral Diseases, Department of Prosthodontics, West China Hospital of Stomatology, Sichuan University, Chengdu 610041, Sichuan, China.

[b]College of Polymer Science and Engineering, State Key Laboratory of Polymer Materials Engineering, Sichuan University, Chengdu 610065, China.

[c]State Key Laboratory of Oral Diseases, National Center for Stomatology, National Clinical Research Center for Oral Diseases, West China Hospital of Stomatology, Sichuan University, Chengdu 610041, Sichuan, China.

[d]Med-X Center for Materials, Sichuan University, Chengdu, 610041, China

*Email: leelei@scu.edu.cn

Table S1. Proportion of different components in the prepolymer solution.

Sample	GelMA %	SA %	$MgCl_2$ %	PEGDA %	nHA %	LAP %
5G1S	5	1	--	--	--	0.5
5G2S	5	2	--	--	--	0.5
5G3S/GS	5	3	--	--	--	0.5
GS@Mg	5	3	1.5	--	--	0.5
GP	10	--	--	5	--	0.5
GP@nHA	10	--	--	5	3	0.5

Table S2. Primer sequences used in this study for real-time quantitative PCR (RT-qPCR) analysis.

Gene	**Forward Primer**	**Reverse Primer**
β-actin	AGCCATGTACGTAGCCATCC	CTCTCAGCTGTGGTGGTGAA
Cgrp	AGGTTCCTGCTCAGGGAGG	GCTTCAGAGCCCACATTGGT
Bmp-2	AAGCGTCAAGCCAAACACAAACAG	CCAGTCATTCCACCCCACATCAC
Opn	CCAGCCAAGGACCAACTACA	AGTGTTTGCTGTAATGCGCC
Runx2	CATGGCCGGGAATGATGAG	TGTGAAGACCGTTATGGTCAAAGTG
Ocn	CCGTTTAGGGCATGTGTTGC	TTTCGAGGCAGAGAGAGGGA

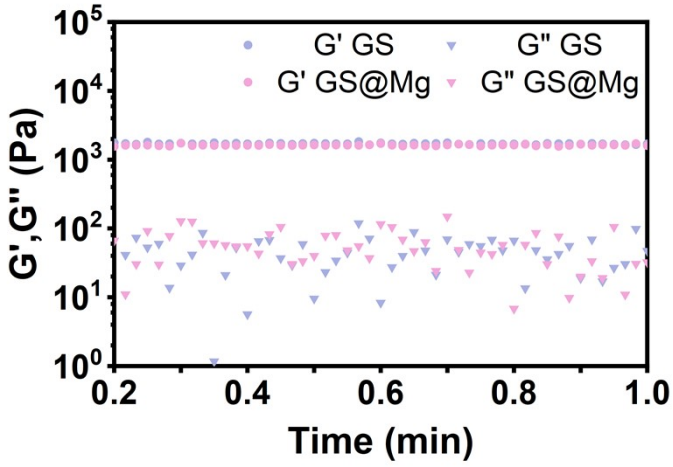

Figure S1 Rheological properties of upper hydrogels in a time-dependent model.

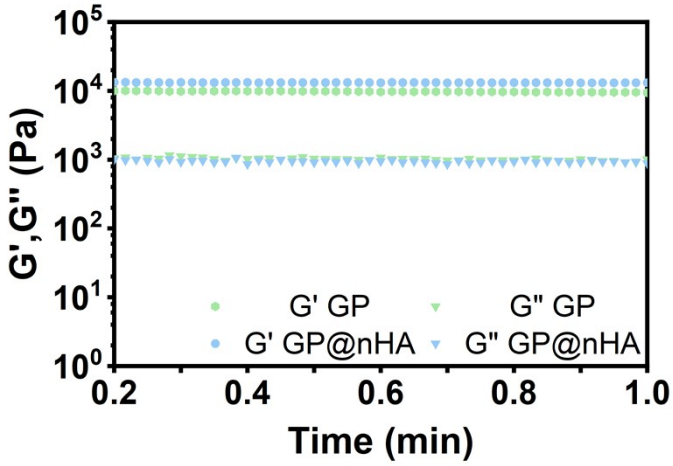

Figure S2 Rheological properties of bottom hydrogels in a time-dependent model.

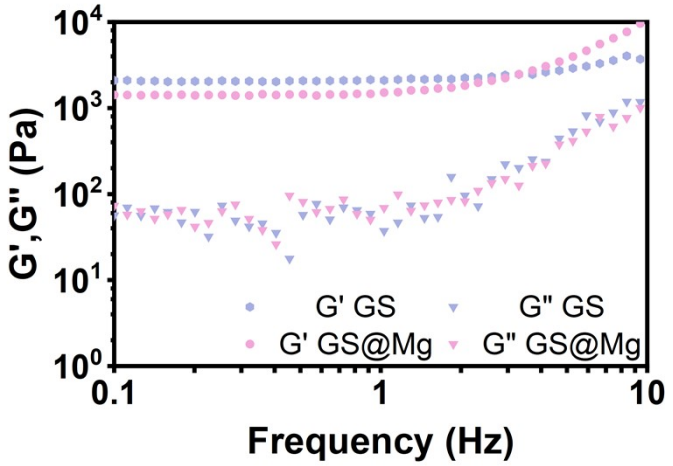

Figure S3 Frequency sweep measurements of upper hydrogels.

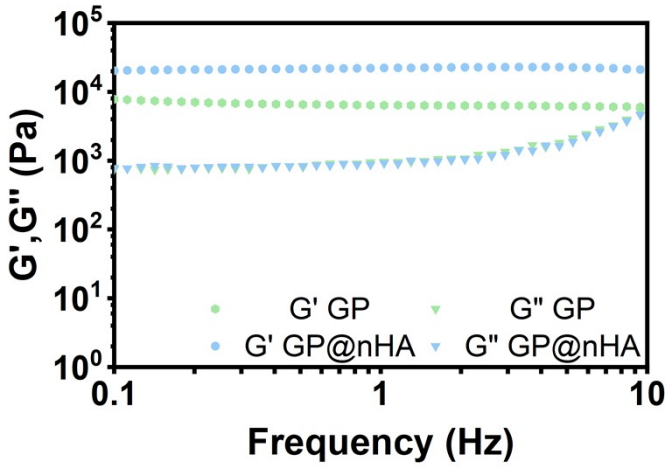

Figure S4 Frequency sweep measurements of bottom hydrogels.

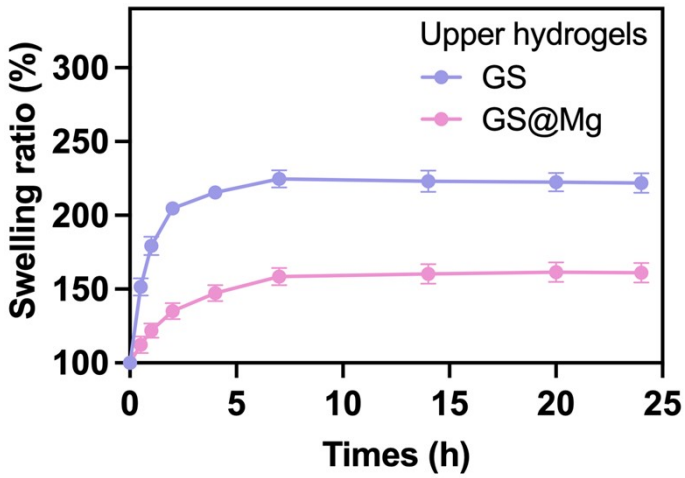

Figure S5 Swelling kinetics of upper hydrogels.

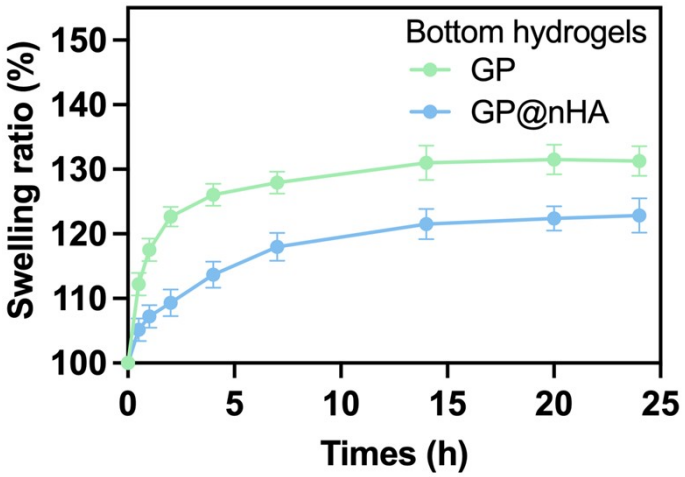

Figure S6 Swelling kinetics of bottom hydrogels.

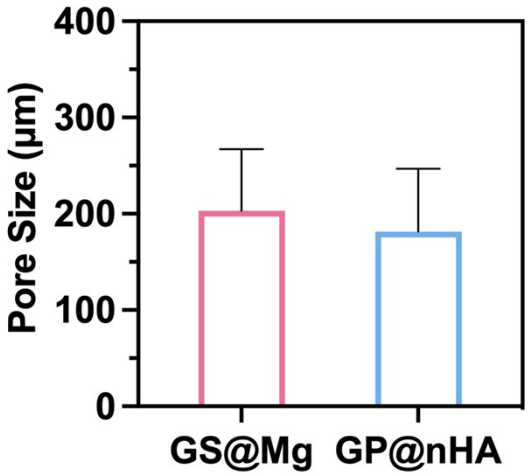

Figure S7 Pore size of GS@Mg and GP@nHA, Error bars represent the standard deviation.

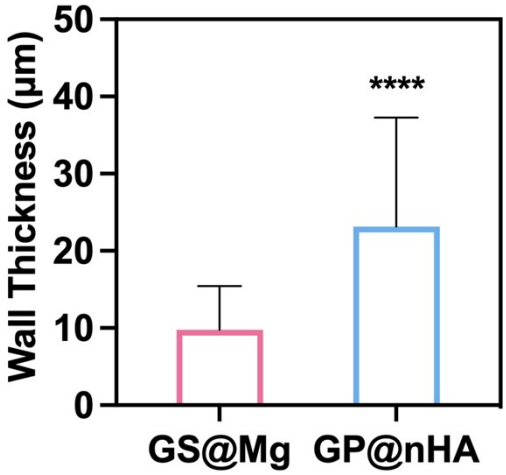

Figure S8 Wall Thickness of GS@Mg and GP@nHA, Error bars represent the standard deviation.

Asterisks indicate p values (*p < 0.05, **p < 0.01, ***p < 0.001, and ****p < 0.0001).

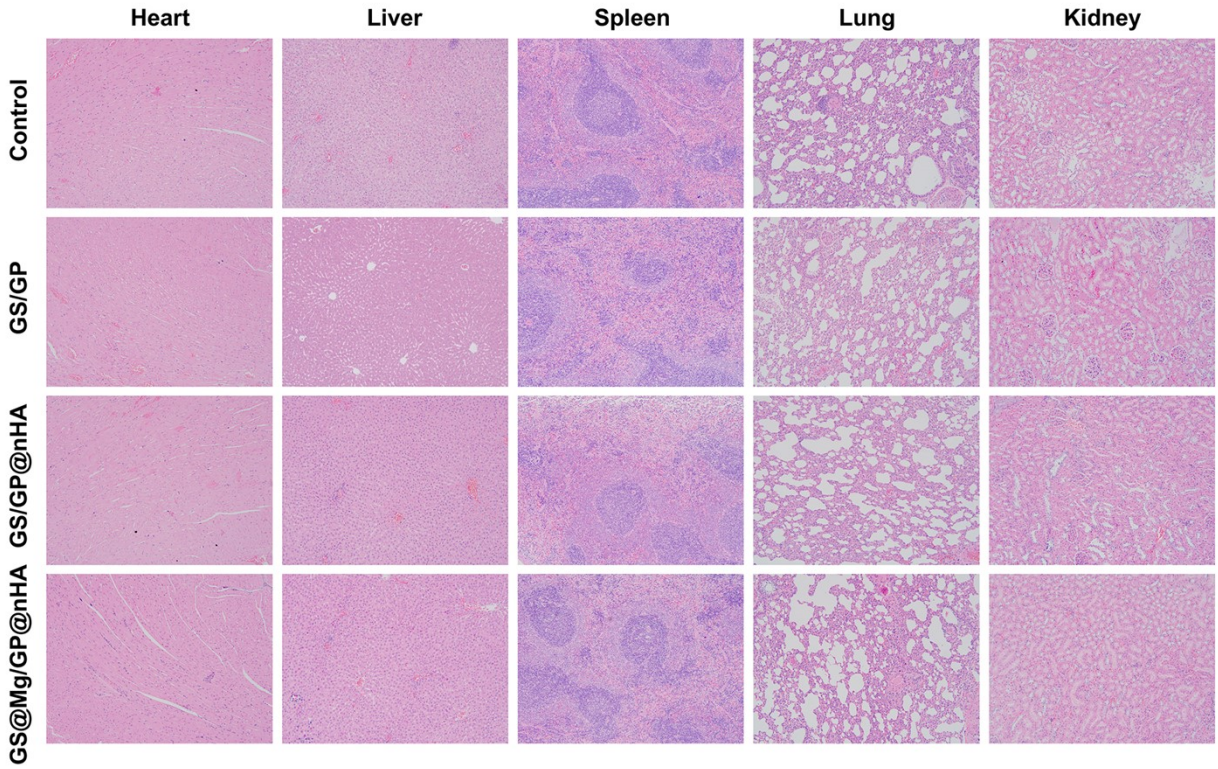

Figure S9 H&E staining of tissue sections of different organs (heart, liver, spleen, stomach, and kidney) after 4 weeks of bilayer hydrogels implantation

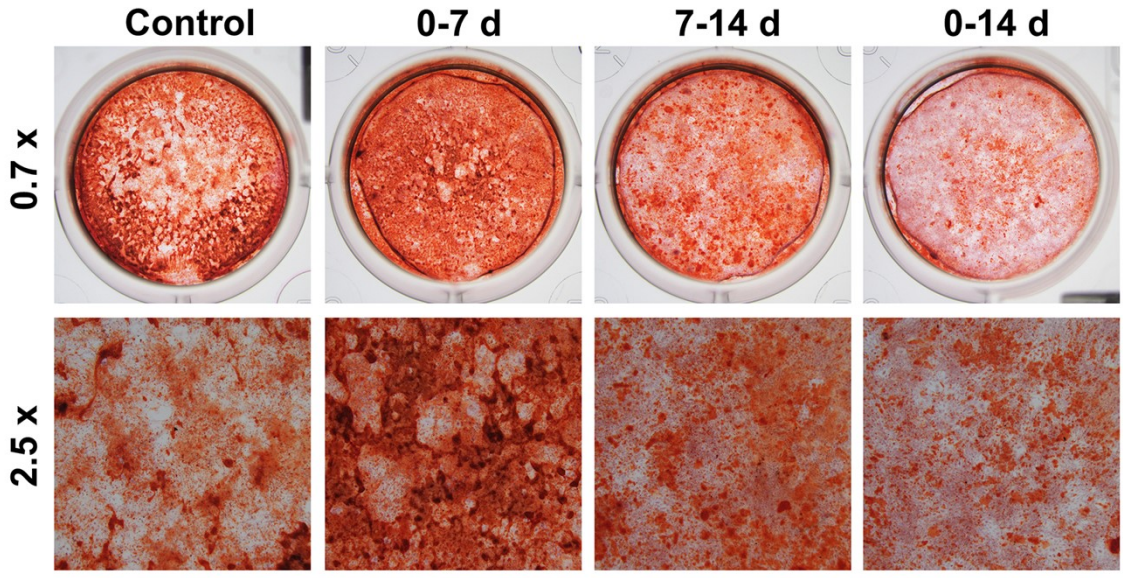

Figure S10 ARS staining after 14 days of osteogenic induction with the addition of 2 mM Mg^{2+} at early (0-7 d), late (7-14 d), and full stages (0-14 d)

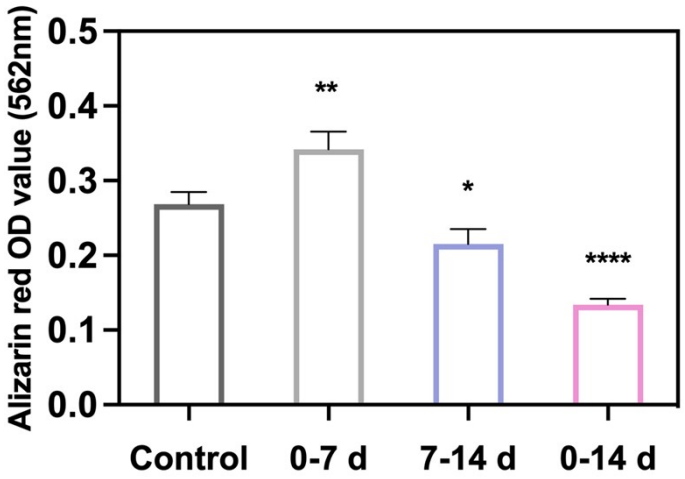

Figure S11. Quantification of ARS staining after 14 days of osteogenic induction with the addition of 2 mM Mg^{2+} at early (0-7 d), late (7-14 d), and full stages (0-14 d), Error bars represent the standard deviation. Asterisks indicate p values (*$p < 0.05$, **$p < 0.01$, ***$p < 0.001$, and ****$p < 0.0001$).

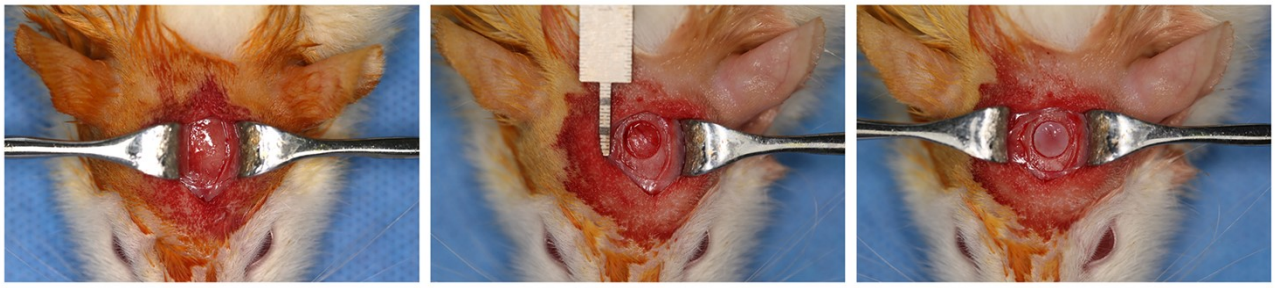

Figure S12. Images of the critical-size bone defect and the implantation of bilayer hydrogel.